Vol. 19, No. 2 (2020) 569-583
Revista Mexicana de Ingeniería Química

Non-competitive $\mathcal{L}_2/\mathcal{D}$ control applied to continuous concentric tubes heat exchangers

Control no-competitivo en $\mathcal{L}_2/\mathcal{D}$ aplicado a intercambiadores de calor de tubos concentricos continuos

R. González-González[1], J.A. Flores-Márquez[1], E. López-Sánchez[1], G.C. Rodríguez-Jimenes[1], J. Carrillo-Ahumada[2] and M.A. García-Alvarado[1]*

[1] *Chemical and Biochemical Engineering Department-UNIDA. Tecnológico Nacional de México Campus Veracruz. Av. Miguel A. de Quevedo 2779. 91860 Veracruz, VER. México.*
[2] *Institute of Applied Chemistry. Universidad del Papaloapan. Circuito Central 200, colonia Parque Industrial. 68301 Tuxtepec, OAX. México.*

Received: June 29, 2019; Accepted: August 31, 2019

Abstract

Non-competitive geometric nature of $\mathcal{L}_2/\mathcal{D}$ controls was shown and its potential was demonstrated by applying $\mathcal{L}_2/\mathcal{D}$ proportional integral (PI) algorithms to continuous concentric tubes heat exchangers (CCTHE) as example of space distributed parameter systems. Both SISO (single input single output) and decentralized MIMO (multiple input multiple output) structures were applied. Dynamic models of CCTHE were expressed in continuous space state. Results show that SISO $\mathcal{L}_2/\mathcal{D}$ PI algorithm applied to the heat exchanger, gives similar performance and robustness with less parameters than previous geometric controls reported in literature. The proposed $\mathcal{L}_2/\mathcal{D}$ PI algorithm was easily extended to decentralized MIMO structure.

Keywords: Optimal control, robust control, geometric control, heat exchangers, distributed parameter process.

Resumen

Se demostraron la naturaleza geométrica no-competitiva de controles en $\mathcal{L}_2/\mathcal{D}$ y su potencial aplicando algoritmos $\mathcal{L}_2/\mathcal{D}$ proporcionales integrales (PI) a intercambiadores de calor de tubos concéntricos en régimen continuo (CCTHE) como ejemplo de sistemas con parámetros distribuidos en el espacio. Se aplicaron estructuras tanto SISO (single input single output) como MIMO (multiple input multiple output) descentralizadas. Los modelos dinámicos de los CCTHE fueron expresados en el espacio de estado continuo. Los resultados muestran que el algoritmo $\mathcal{L}_2/\mathcal{D}$ PI SISO aplicado en intercambiadores de calor, entrega un desempeño y robustez con menos parámetros que controles geométricos reportados en trabajos previos. El control PI en $\mathcal{L}_2/\mathcal{D}$ fue fácilmente extendido a una estructura MIMO descentralizado.

Palabras clave: Control óptimo, control robusto, control geométrico, intercambiadores de calor, procesos con parámetros distribuidos.

1 Introduction

Control theory has experienced an important development in the field of Chemical Engineering (Shih 1969; Tsiligiannis & Svoronos, 1988; Chen *et al*. 2002; Hernández-Martínez *et al*. 2008; Goncalves *et al*. 2008; García *et al*. 2010; Velasco-Pérez *et al*. 2011; Aguilar-Garnica, *et al*. 2011; Estévez-Sánchez *et al*., 2017; Xie *et al*., 2018; Schorsch *et al*., 2019). One of the control theory concepts, that has been developed within the chemical engineering field, is the $\mathcal{L}_2/\mathcal{D}$ control which has been successfully applied in distillation columns (Ruiz-López *et al*., 2006; García-Avarado & Ruiz-López, 2010), chemical reactors (Carrillo-Ahumada *et al*., 2011), continuous stirred tank heat exchangers (Vargas-González *et al*., 2014) and even aeronautical systems (Carrillo-Ahumada *et al*., 2015). Vargas-González *et al*. 2014 introduced the non-competitive $\mathcal{L}_2/\mathcal{D}$ control as a control in which the error signal and action control deviations are elements of Lebesgue spaces ($\mathcal{L}_2$) and the close loop characteristic matrix eigenvalues are in a limited region ($\mathcal{D}$) of left complex semi-plane.

* *Corresponding author. E-mail*: miguelg@itver.edu.mxx
https://doi.org/10.24275/rmiq/Sim669
issn-e: 2395-8472

Ruiz-López *et al*. (2006) demonstrated that $\mathcal{D}$ criterion implies control robustness and Voßwinkel *et al*. (2019) demonstrated that $\mathcal{D}$ criterion is a damping boundary of controls. $\mathcal{L}_2/\mathcal{D}$ controls include SISO or MIMO (centralized or decentralized) PI or PID algorithms that can be tuned directly from process state-space (García-Avarado & Ruiz-López, 2010; Carrillo-Ahumada *et al*., 2011; Carrillo-Ahumada *et al*., 2015; Estévez-Sánchez *et al*., 2017). In present day, although very complex control algorithms have been developed, the research on mathematical properties and applications of PI or PID algorithms continue both in Laplace dominion (Ma *et al*., 2019; Kozakova *et al*., 2019) and in state-space dominion (Voßwinkel *et al*., 2019). State-space has particular interest because is commonly used for dynamic modeling of chemical engineering processes (Alzate-Ibanez 2018; Bolaños-Reynoso *et al*., 2018; Martínez-Monteagudo 2018). Although the $\mathcal{L}_2/\mathcal{D}$ control has been applied in distillation columns, columns dynamics models have been obtained by process identification techniques and they have been represented as transfer functions with time delay (Ruiz-López *et al*., 2006; Estévez-Sánchez *et al*., 2017). However, time delay is only an approximation of the real behavior of distillation columns (Juarez-Romero *et al*., 2010). The dynamic of distillation columns (with plates of with packed bed) must be represented as a series of N ordinary differential equations (assuming ideal fixed units in the case of packed bed) that increase the order of any representation in Laplace dominion and therefore time delay has been used for to simplify the order. Any space distributed parameter process present the same high order problem. Others typical examples of distributed parameter process are the continuous concentric tubes heat exchanger (CCTHE). Heat exchangers optimal control has been studied at least since Shih (1969). Recently Aguilar-Garnica *et al*. (2011) applied a PI to a CCTHE; and, Maidi *et al*. (2009) used boundary geometric control for CCTHE two SISO controls. PI non-competitive $\mathcal{L}_2/\mathcal{D}$ algorithm represents a potential optimal-robust control for CCTHE because it can handle high order systems directly from the space-state. Therefore, this work has two mains objectives: the geometrical formalization of non-competitive $\mathcal{L}_2/\mathcal{D}$ controls in order to show their complete potential; and, the application of PI algorithms organized as non-competitive $\mathcal{L}_2/\mathcal{D}$ optimal-robust controls for CCTHE in both SISO and MIMO configurations as example of high order systems.

2 Modeling

2.1 $\mathcal{L}_2/\mathcal{D}$ controls formalization

Resuming the concepts expressed in previous works (Ruiz-López *et al*., 2006; García-Avarado & Ruiz-López, 2010; Carrillo-Ahumada *et al*., 2011; Vargas-González *et al*., 2014), a non-competitive $\mathcal{L}_2/\mathcal{D}$ control is defined in Eqs. (1) to (7),

$$min\ I(\alpha,\beta_1,\beta_2,\gamma,\delta_1,\delta_2) = \int_0^\infty e' Qedt + \int_0^\infty u_d' Ru_d dt \tag{1}$$

Subject to

$$\lambda_i : \{|\mathbf{I}\lambda_i - \mathbf{A}| = 0\} \in \mathcal{D} \quad \forall i = 1,2,\ldots,(n+k)$$

$$\mathcal{D} \subset C_- = \{z : \Im(z)/\Re(z) < \phi\} \tag{2}$$

where $e = r - y \in \mathcal{R}^r$, $u_d = u - u_\infty \in \mathcal{R}^c$ and,

$$\frac{dx}{dt} = Ax + B_1 w + B_2 u \tag{3}$$

$$y = Cx + D_1 w + D_2 u \tag{4}$$

$$\frac{d\xi}{dt} = \alpha\xi + \beta_1 r + \beta_2 y \tag{5}$$

$$u = \gamma\xi + \delta_1 r + \delta_2 y \tag{6}$$

$$u_\infty = \lim_{t\to\infty} u \tag{7}$$

for $I : \mathcal{R}^r \times \mathcal{R}^c \to \mathcal{R}$ is a quadratic performance index, $x \in \mathcal{R}^n$ is the state space, y is the control algorithm state space, $w \in \mathcal{R}^m$ is the vector of output variables, u is the vector of the input variables, r is the vector of control variables, and is the vector of the set point. $Q \in \mathcal{R}^{n\times n}$ and $Q \in \mathcal{R}^{c\times c}$ are weight matrices; $A \in \mathcal{R}^{n\times n}$, $B_1 \in \mathcal{R}^{n\times n}$, $B_2 \in \mathcal{R}^{n\times c}$, $C \in \mathcal{R}^{r\times n}$, $D_1 \in \mathcal{R}^{r\times c}$, $D_2 \in \mathcal{R}^{r\times c}$, $\alpha \in \mathcal{R}^{k\times k}$, $\beta_1 \in \mathcal{R}^{k\times r}$, $\beta_2 \in \mathcal{R}^{k\times r}$, $\gamma \in \mathcal{R}^{c\times k}$, $\delta_1 \in \mathcal{R}^{c\times r}$ and $\delta_2 \in \mathcal{R}^{c\times r}$ are the process and control parameters matrices. $\mathbf{A}$ is the close loop characteristic matrix when Eqs. (3) to (6) are expressed as,

$$\frac{d\mathbf{X}}{dt} = \mathbf{A}\mathbf{X} + \mathbf{B}_1 w + \mathbf{B}_2 r \tag{8}$$

$$y = \mathbf{C}_1\mathbf{X} + \mathbf{D}_{11} w + \mathbf{B}_{12} r \tag{9}$$

$$u = \mathbf{C}_2\mathbf{X} + \mathbf{D}_{21}w + \mathbf{D}_{22}r \tag{10}$$

where $\mathbf{X}' = [x'\xi']$ and (García-Alvarado & Ruiz-López 2010),

$$\mathbf{A} = \begin{bmatrix} A + B_2\delta_2\Delta_1 C & B_2\Delta_2\delta \\ \beta_2\Delta_1 C & \alpha + \beta_2\Delta_1\gamma \end{bmatrix}$$

$$\mathbf{B}_1 = \begin{bmatrix} B_1 + B_2\delta_2\Delta_1 D_1 \\ \beta_2\Delta_1 D_1 \end{bmatrix} \quad \mathbf{B}_2 = \begin{bmatrix} B_2\Delta_2\delta_1 \\ \beta_1 + \beta_2\Delta_1 D_2\delta_1 \end{bmatrix}$$

$$\mathbf{C}_1 = \begin{bmatrix} \Delta_1 C\Delta_1 D_2\gamma \end{bmatrix} \quad \mathbf{C}_2 = \begin{bmatrix} \delta_2\Delta_1 C\Delta_2\gamma \end{bmatrix}$$

$$\mathbf{D}_{11} = \Delta_1 D_1 \quad \mathbf{D}_{12} = \Delta_1 D_2\delta_1 \quad \mathbf{D}_{21} = \delta_2\Delta_1 D_1$$
$$\mathbf{D}_{22} = \Delta_2\delta_1 \quad \Delta_1 = (\mathbf{I} - D_2\delta_2)^{-1} \quad \Delta_2 = \mathbf{I} - \delta_2\Delta_1 D_2$$

It was demonstrated (Vargas-González *et al.*, 2014) that if α has at least c eigenvalues zeros then $\left(\int_0^\infty e'Qedt + \int_0^\infty u_d'Ru_d dt\right)^{1/2} \in \mathcal{R}$, and therefore is an element of a Lebesgue space ($\mathcal{L}_2$), which implies that it can be analytically evaluated under step $(1(t)K)$ inputs as follows,

$$I_e = \int_0^\infty e'Qedt = K'\mathbf{B}_2'P_y\mathbf{B}_2K \quad for\ w = 0,\ r = 1(t)K \tag{11}$$

$$I_u = \int_0^\infty u_d'Ru_d dt = K'\mathbf{B}_2'P_u\mathbf{B}_2K \quad for\ w = 0,\ r = 1(t)K \tag{12}$$

where P_y and P_u were the solutions of the following Riccati equations,

$$\mathbf{A}'P_y + P_y\mathbf{A} - \left(\mathbf{A}^{-1}\right)\mathbf{C}_1'Q\mathbf{C}_1\left(\mathbf{A}^{-1}\right) = 0 \tag{13}$$

$$\mathbf{A}'P_y + P_y\mathbf{A} - \left(\mathbf{A}^{-1}\right)\mathbf{C}_2'R\mathbf{C}_2\left(\mathbf{A}^{-1}\right) = 0 \tag{14}$$

It is important to take into account that a geometric control is defined as the solution of the following optimization problem (Boscani & Piccoli 1998),

$$\frac{dx}{dt} = f(x,u) \quad x \in M \quad u \in U \tag{15}$$

$$min\left(\int \mathcal{N}(x,u)dt + \varphi(x_\infty)\right) \tag{16}$$

where, M is a manifold, U is a metric space, $F : M \times U \to M$, $\mathcal{N} : M \times U \to \mathcal{R}$, and $\varphi : M \to \mathcal{R}$. That is, a geometric control is an optimal control in which the control action applied to a smooth process state space x, minimize the integral of a positive norm $\mathcal{N}$. Therefore, the mathematical characteristics of non-competitive $\mathcal{L}_2/\mathcal{D}$ control are defined in the following remarks,

Remark 1 □ *$e'Qe + u_d'Ru_d = \mathcal{N}(x,u)$. That is, the square sum of error elements plus the square sum of control action deviation is a feasible positive norm function of x and u. Therefore, $I = \int_0^\infty e'Qedt + \int_0^\infty u_d'Ru_d dt$ is a particular form of $\int \mathcal{N}(x,u)dt + \varphi(x_\infty)$. As consequence, if A, B_2, B_2, C, D_1, D_2 are constants (Eqs 3 and 4 are linear with constant coefficients) then $x \in M$ and $\mathcal{L}_2/\mathcal{D}$ control defined in Eqs. (1) to (16) is a class of parametric geometric control with $\alpha,\beta_1,\beta_2,\gamma,\delta_1,\delta_2$ as parameters.* □

Remark 2 □ *The concept of control action deviation square integral $\left(\int_0^\infty u_d'Ru_d dt\right)$ introduced in our previous work (Vargas-González et al., 2014) and demonstrated as theorem 1 of appendix A, guaranties that a control action integral was element of $\mathcal{L}_2$ (Eq. 12) at difference of typical control action square integral $\left(\int_0^t fu'Rudt\right)$ (García-Avarado & Ruiz-López, 2010). This concept has the decisive consequence that $\int_0^\infty e'Qedt$ vs $\int_0^\infty u_d'Ru_d dt$ are non-necessarily competitive because in optimum neighborhood (Eq. 1), increasing control actions deviations may produce an increasing in error signals.* □

Remark 3 □ *If exists a set of $\alpha,\beta_1,\beta_2,\gamma,\delta_1,\delta_2$ for which $\Sigma < 0$ (where Σ is the spectral abscise or $\Sigma = max\Re(\lambda_i)$ for $\lambda_i : \{|\mathbf{I}\lambda_i - \mathbf{A}| = 0\}\ \forall i = 1,2,\ldots,(n+k)$) then would be Hurwitz and Eqs. (13) and (14) would have real P_y and P_u solutions for Q and R positive defined. As consequence $I \in \mathcal{L}_2$ and the system (3) to (6) will be stabilizable and controllable.* □

Remark 4 □ *Like I is in terms of e and u_d the optimization problem defined in Eqs. (1) and (2) does not require that system must be observable. That is, it is not necessary rebuild x from y.* □

Remarks 1-4 state that $\mathcal{L}_2/\mathcal{D}$ controls defined in Eqs. (1) to (4) are linear controls that can be optimized simultaneously in error signals and control action (the essence of non-competitiveness), with robustness, damping limited (by $\mathcal{D}$ criterion), with enough parameters for to be controllable and stabilizable; and, without the necessity that systems

must be observable. These mathematical properties are especially useful for linear controllers of high order systems as continuous concentric tubes heat exchanger (CCTHE).

2.2 CCTHE dynamic modeling

A typical counter current CCTHE may be modeled with heat balances in complete mixed volume elements V_{cj} (in cold tube) and V_{hj} (in heat tube),

$$\rho Cp V_{cj}\frac{dT_{cj}}{dt} = q_c\rho Cp\left(T_{cj-1}-T_{cj}\right)+ha\left(T_{hj}-T_{cj}\right)V_{cj} \tag{17}$$

$$\rho Cp V_{hj}\frac{dT_{hj}}{dt} = q_h\rho Cp\left(T_{hj-1}-T_{hj}\right)+ha\left(T_{hj}-T_{cj}\right)V_{hj} \tag{18}$$

where $j = 1,2,\ldots,N$, N is the number of ideal mixed elements (if $N = 1$ is a completely mixed process; if $N \to \infty$ is a plug flow process); ρ fluid density; Cp fluid heat capacity; T_c cold fluid temperature, T_h hot fluid temperature, q_c cold fluid flow; q_h hot fluid flow; h overall heat transfer coefficient. The average specific surface is,

$$a = 4/\left((d_0+d_{01})/2\right) \tag{18a}$$

where d_0 is internal tube internal diameter; d_{01} is internal tube external diameter. Ideally mixed units volumes are,

$$V_{cj} = \left(\pi d_0^2/4\right)L_j \tag{18b}$$

$$\text{and}\quad V_{hj} = \pi\left(d_1^2/4 - d_{01}^2/4\right)L_j \tag{18c}$$

$$\text{with}\quad L_j = L/N \tag{18d}$$

where L is heat exchanger total length.

2.3 Linearized state space

Eqs. (17) and (18) represent a non-linear system of differential equations. This system may be represented by linear state space (Eqs. 3 and 4) expanding in Taylor series around the steady state. The results are,

$$x' = \left[T_{c1}T_{c2}\cdot\cdot T_{cN}T_{h1}T_{h2}\cdot\cdot T_{hN}\right]$$

$$y' = \left[T_{cN}T_{h1}\right] \quad u' = \left[T_{hN+1}q_h\right]$$

$$A = \begin{bmatrix}A_{11}A_{12}\\A_{21}A_{22}\end{bmatrix} \quad B_2 = \begin{bmatrix}B_{211}B_{212}\\B_{221}B_{222}\end{bmatrix} \quad C = \begin{bmatrix}C_{11}C_{12}\\C_{21}C_{22}\end{bmatrix}$$

$$D_2 = \left[0\right] \tag{19}$$

$$A_{11} = \begin{bmatrix} -\frac{q_{cs}}{V_{c1}}-\frac{ha}{\rho Cp} & 0 & 0 & \cdot & \cdot & 0 & 0\\ \frac{q_{cs}}{V_{c2}} & -\frac{q_{cs}}{V_{c2}}-\frac{ha}{\rho Cp} & 0 & \cdot & \cdot & 0 & 0\\ \cdot & \cdot & \cdot & & & \cdot & \cdot\\ \cdot & \cdot & \cdot & & & \cdot & \cdot\\ 0 & 0 & 0 & \cdot & \cdot & \frac{q_{cs}}{V_{cN}} & -\frac{q_{cs}}{V_{cN}}-\frac{ha}{\rho Cp}\end{bmatrix}$$

$$A_{12} = \begin{bmatrix}\frac{ha}{\rho Cp} & 0 & \cdot & \cdot & 0\\ 0 & \frac{ha}{\rho Cp} & \cdot & \cdot & 0\\ \cdot & \cdot & & & \cdot\\ \cdot & \cdot & & & \cdot\\ 0 & 0 & \cdot & \cdot & \frac{ha}{\rho Cp}\end{bmatrix} \qquad A_{21} = \begin{bmatrix}\frac{ha}{\rho Cp} & 0 & \cdot & \cdot & 0\\ 0 & \frac{ha}{\rho Cp} & \cdot & \cdot & 0\\ \cdot & \cdot & & & \cdot\\ \cdot & \cdot & & & \cdot\\ 0 & 0 & \cdot & \cdot & \frac{ha}{\rho Cp}\end{bmatrix}$$

$$A_{22} = \begin{bmatrix} -\frac{q_{hs}}{V_{h1}}-\frac{ha}{\rho Cp} & \frac{q_{hs}}{V_{h1}} & 0 & \cdot & \cdot & 0 & 0\\ 0 & -\frac{q_{hs}}{V_{h2}}-\frac{ha}{\rho Cp} & \frac{q_{hs}}{V_{h2}} & \cdot & \cdot & 0 & 0\\ \cdot & \cdot & \cdot & & & \cdot & \cdot\\ \cdot & \cdot & \cdot & & & \cdot & \cdot\\ 0 & 0 & 0 & \cdot & \cdot & 0 & -\frac{q_{hs}}{V_{hN}}-\frac{ha}{\rho Cp}\end{bmatrix}$$

$$B_{211} = \begin{bmatrix} 0 \\ 0 \\ \cdot \\ \cdot \\ 0 \end{bmatrix} \quad B_{212} = \begin{bmatrix} 0 \\ 0 \\ \cdot \\ \cdot \\ 0 \end{bmatrix} \quad B_{221} = \begin{bmatrix} 0 \\ 0 \\ \cdot \\ \cdot \\ \frac{q_{hs}}{V_{hN}} \end{bmatrix} \quad B_{222} = \begin{bmatrix} \frac{T_{hN+1s}}{V_{h1}} \\ \frac{T_{hN+1s}}{V_{h1}} \\ \cdot \\ \cdot \\ \frac{T_{hN+1s}}{V_{h1}} \end{bmatrix} \quad C_{11} = \begin{bmatrix} 0 & 0 & \cdot & \cdot & 1 \end{bmatrix}$$

$$C_{12} = \begin{bmatrix} 0 & 0 & \cdot & \cdot & 0 \end{bmatrix} \quad C_{21} = \begin{bmatrix} 0 & 0 & \cdot & \cdot & 0 \end{bmatrix} \quad C_{22} = \begin{bmatrix} 0 & 0 & \cdot & \cdot & 0 \end{bmatrix} \tag{20}$$

Matrices (20) definition considers a general case in where the process outputs (target variables) are the cold temperature (T_{cN}) at volume N (the output cold temperature) and the hot temperature (T_{h1}) at volume 1 (the output hot temperature in counter current). And the handle variables for control are the input hot temperature (T_{hN+1}) and flow of hot temperature fluid (q_h). The subscript indicates the variable value at steady state.

2.4 PI algorithm state space

As it was detailed in introduction section, a PI algorithm can be organized as a non-competitive $\mathcal{L}_2/\mathcal{D}$ control. In the case of decentralized MIMO PI, for CCTHE represented by Eqs. (3) and (4) and matrices (19) and (20), it may be expressed in terms of Eqs. (5) and (6) with the following matrices,

$$\alpha = \begin{bmatrix} \alpha_{11} & \alpha_{12} \\ \alpha_{21} & \alpha_{22} \end{bmatrix} \quad \beta_1 = \begin{bmatrix} \beta_{111} & \beta_{112} \\ \beta_{121} & \beta_{122} \end{bmatrix} \quad \beta_2 = \begin{bmatrix} \beta_{211} & \beta_{212} \\ \beta_{221} & \beta_{222} \end{bmatrix}$$

$$\gamma = \begin{bmatrix} \gamma_{11} & \gamma_{12} \\ \gamma_{21} & \gamma_{22} \end{bmatrix} \quad \delta_1 = \begin{bmatrix} \delta_{111} & \delta_{112} \\ \delta_{121} & \delta_{122} \end{bmatrix} \quad \delta_2 = \begin{bmatrix} \delta_{211} & \delta_{212} \\ \delta_{221} & \delta_{222} \end{bmatrix} \tag{21}$$

$$\alpha_{ij} = 0,\ \beta_{1ij} = 1,\ \beta_{2ij} = -1,\ \gamma_{ij} = K_{iij},\ \delta_{1ij} = K_{pij},\ \delta_{2ij} = -K_{pij}. \tag{22}$$

In the case of SISO PI algorithm systems can be represented with the same matrix structure (19)-(20) and the following modifications:

1. SISO PI with hot temperature T_{hN+1} as handle variable for control and cold temperature output T_{cN} as target variable,

$$A = \begin{bmatrix} A_{11} & A_{12} \\ A_{21} & A_{22} \end{bmatrix} \quad B_2 = \begin{bmatrix} B_{211} \\ B_{221} \end{bmatrix}$$

$$C = \begin{bmatrix} C_{11} & C_{12} \end{bmatrix} \quad D_2 = \begin{bmatrix} 0 \end{bmatrix}$$

$$\alpha_{11} = 0\ \beta_1 = \beta_{111}\ \beta_2 = \beta_{211}\ \gamma = \gamma_{11}\ \delta_1 = \delta_{111}\ \delta_2 = \delta_{211}. \tag{23}$$

2. SISO PI with hot fluid flow q_h as handle variables for control and cold temperature output T_{cN} as target variable,

$$A = \begin{bmatrix} A_{11} & A_{12} \\ A_{21} & A_{22} \end{bmatrix} \quad B_2 = \begin{bmatrix} B_{121} \\ B_{222} \end{bmatrix}$$

$$C = \begin{bmatrix} C_{11} & C_{12} \end{bmatrix} \quad D_2 = \begin{bmatrix} 0 \end{bmatrix}$$

$$\alpha_{22} = 0\ \beta_1 = \beta_{122}\ \beta_2 = \beta_{222}\ \gamma = \gamma_{22}\ \delta_1 = \delta_{122}\ \delta_2 = \delta_{222}. \tag{24}$$

In order to compare the non-competitive geometric $\mathcal{L}_2/\mathcal{D}$ PI algorithm, Maidi *et al*. (2009) geometric SISO controls were taken as reference. Maidi *et al*. (2009) used a different modeling criterion. They modeled the dynamic of a counter current CCTHE with,

$$\frac{\partial T_c}{\partial t} = -\nu_c \frac{\partial T_c}{\partial z} + a_c(T_h - T_c) \tag{25}$$

$$\frac{\partial T_h}{\partial t} = -\nu_h \frac{\partial T_h}{\partial z} + a_h(T_h - T_c) \tag{26}$$

where ν_c cold fluid velocity, ν_h hot fluid velocity, a_c cold fluid heat transfer constant, a_h hot fluid heat transfer constant, $0 < z < L$ linear coordinate within heat exchanger. And the following control laws,

$$u = T_h|_{z=L} = \frac{1}{a_c}\left[\frac{1}{\tau}(\mu - T_c|_{z=L}) - \nu \left.\frac{\partial T_c}{\partial z}\right|_{z=L} + a_c\, T_c|_{z=L}\right] \tag{27}$$

$$u = \nu_h = \frac{1}{a_c\beta_2 \left.\frac{\partial T_h}{\partial z}\right|_{z=L-\varepsilon}}\left[\mu - \beta_2\nu_c \left.\frac{\partial^2 T_c}{\partial z^2}\right|_{z=L-\varepsilon} + \beta_2 a_c \nu_c \left.\frac{\partial T_h}{\partial z}\right|_{z=L-\varepsilon}\right.$$

$$\left. - (2\beta_2 a_c\nu_c - \beta_1\nu_c) \left.\frac{\partial T_c}{\partial z}\right|_{z=L-\varepsilon} + \left(\beta_2 a_c^2 + \beta_2 a_c a_h - \beta_1 a_c\right)(T_h|_{z=L-\varepsilon} - T_c|_{z=L-\varepsilon}) - T_c|_{z=L-\varepsilon}\right] \tag{28}$$

$$\mu = K_p\left[(r - T_c|_{z=L}) + \frac{1}{\tau_i}\int_0^t (r - T_c|_{z=L})\,dt\right] \tag{29}$$

Eq. (27) is the control law for a SISO system with inlet hot temperature as handle variable, and Eq. (28) is the control law for a SISO system with inlet hot fluid velocity as handle variable. In both cases μ is calculated from a PI algorithm (Eq. 29) with outlet cold temperature as target variable. Maidi *et al*. (2009) calculated the control parameters by geometrics technics (not detailed). Eqs. (25) and (26) discretized in ∂z, and linearized by Taylor series expansion, may be represented with matrix structures (19) and (20) with the following modifications: matrix A_{11} diagonal elements $-\frac{\nu_{cs}}{L_j} - a_c$; matrix A_{11} non-diagonal elements $\frac{\nu_{cs}}{L_j}$; matrix A_{12} elements a_c; matrix A_{22} diagonal elements $-\frac{\nu_{hs}}{L_j} - a_h$; matrix A_{22} non-diagonal elements $\frac{\nu_{hs}}{L_j}$; matrix A_{21} elements a_h. B_{221} matrix element $\frac{\nu_{hs}}{L_N}$; B_{221} matrix elements $\frac{T_{hN+1s}}{L_1}$.

3 Methodology

The tuning method of a PI algorithm as a non-competitive $\mathcal{L}_2/\mathcal{D}$ geometric control is the solution of the problem defined by Eqs. (1)-(7) with matrices (19)-(20) for CCTHE linearized state-space, and matrices (21)-(22) for decentralized MIMO PI, or matrices (23)-(24) for SISO PI. This problem was solved in three steps. Every one of the following steps was solved with the Box-Ruiz-Rodríguez-García optimization algorithm (Ruiz-López *et al*., 2006), due to its capacity for finding solution in non-convex valid regions without derivatives of target function.

3.1 Initialization

The following problem must be solved,

$$min\Sigma(\alpha,\beta_1,\beta_2,\gamma,\delta_1,\delta_2) \tag{30}$$

where

$$\Sigma = max\Re(\lambda_i)\ \ \lambda_i : \{|\mathbf{I}\lambda_i - \mathbf{A}| = 0\}\ \ \forall_i = 1,2,\ldots,(n+k)$$

That is, the problem is minimize the spectral abscise (Σ) of the close loop control system as function of parameters $\alpha,\beta_1,\beta_2,\gamma,\delta_1,\delta_2$ in real domain. A negative solution (a stable control system) is required. If the case of PI algorithm, only γ,δ_1,δ_2 elements are search, because α,β_1,β_2 are constant in agreement with Eqs. (21) and (22). In agreement with remark 3, if this step produces a negative value for Σ the system is stabilizable and controllable.

3.2 Searching for and adequate geometric space $\mathcal{D}$

The following problem must be solved with the solution of 3.1. as initial guess,

$$min\phi(\alpha,\beta_1,\beta_2,\gamma,\delta_1,\delta_2) \tag{31}$$

where

$$\phi = max(\Im(\lambda_i)/\Re(\lambda_i))\ \ \lambda_i : \{|\mathbf{I}\lambda_i - \mathbf{A}| = 0\}\ \ \forall_i = 1,2,$$

subject to

$$\Sigma < \Sigma_{max}$$

That is, the problem is to find the limit value of ϕ that delimitates the geometric space $\mathcal{D}$ keeping

the control system spectral abscise ($\mathcal{D}$) below of a given negative value ($\mathcal{D}_{max}$) which evidently must be greater that the values obtained in 3.1. The parameters obtained at the solution were used to evaluate the integrals (11) and (12) with Q and R as identity matrixes. The results lead an adequate value for with Q and R in order that two integrals have similar metric. This step produces an adequate reference damping boundary (ϕ) for the control problem in agreement with Voßwinkel *et al*. (2019).

3.3 Solving the $\mathcal{L}_2/\mathcal{D}$ problem

Taking the solution of 3.2. problem as initial guess, and the adequate values for Q and R, the problem defined in Eqs. (1) and (2) must be solved. The problem must relax the ϕ value, that is, constrain for ϕ must be greater than the value obtained in problem 3.2.

4 Results and discussion

4.1 SISO control with input hot fluid temperature as control handle variable

Maidi *et al*. (2009) reported the CCTHE defined with Eqs. (25) and (26) and the following parameters: $a = 2.92s^{-1}$, $v_c = 1m \cdot s^{-1}$, $a_h = 5s^{-1}$, and $L = 1m$; and steady state variables; $v_{hs} = 2m \cdot s^{-1}$, $T_{c0s} = 25$ ºC and $T_{h101s} = 50$ ºC. In order to represent Eqs. (25) and (26) in continuous space state the following discretization was introduced,

$$\frac{dT_{cj}}{dt} = -v_c \frac{T_{cj} - T_{cj-1}}{L_j} + a_c\left(T_{hj} - T_{cj}\right) \tag{32}$$

$$\frac{dT_{hj}}{dt} = -v_h \frac{T_{hj} - T_{hj-1}}{L_j} + a_h\left(T_{hj} - T_{cj}\right) \tag{33}$$

where $j = 1,2,\ldots,N$. The space state was obtained for $N = 20$, which produces that $A \in R^{40\times40}$ with the elements detailed at the end of section 2. It is important to remark that the proposed $\mathcal{L}_2/\mathcal{D}$ requires only 2 parameters and it does not require the evaluation of a first derivative like in Eq. (27). The geometric control characteristics (for Eqs. 27 and 29) tuning by Maidi *et al*., (2009) and the $\mathcal{L}_2/\mathcal{D}$ PI control characteristics (for matrices 23) tuning by procedure described in section 3 are listed in Table 1. The simulation of the process control was obtained with Eqs. (32) and (33) with $N = 100$. That is, the number of ideal mixed elements used for $\mathcal{L}_2/\mathcal{D}$ control tuning ($N = 20$) was different than those used for process simulation ($N = 100$). The 200 ODEs of Eqs (32) and (33) were initially solved, by four order Runge-Kutta method, until reach steady state in order to calculate T_{cjs} and T_{hjs}. Finally the process control simulation were performed solving (by four order Runge-Kutta method) the 200 ODEs (Eqs. 32 and 33) simultaneously with the following control equations, Maidi *et al*., (2009) geometric control (from Eqs. 27 and 29),

$$\frac{d\xi}{dt} = r - (T_{c100} + \eta) \; (therefore, \; \xi \; is \; the \; integral \; of \; error) \tag{34}$$

$$\mu = K_p\left[(r - (T_{c100} + \eta)) + \frac{1}{\tau_i}\xi\right] \tag{35}$$

$$T_{h101} = \frac{1}{a_c}\left[\frac{1}{\tau}(\mu - (T_{c100} + \eta)) - v\frac{(T_{c100} + \eta) - (T_{c95} + \eta)}{5\Delta z} + a_c(T_{c100} + \eta)\right] \tag{36}$$

$\mathcal{L}_2/\mathcal{D}$ control (Eqs. 5 and 6 with matrices 23),

$$\frac{d\xi}{dt} = r - (T_{c100} + \eta) \tag{37}$$

$$T_{h101} = T_{h101s} + K_{p11}(r - (T_{c100} + \eta)) + K_{i11}\xi \tag{38}$$

And the following inputs:

$$r = \begin{cases} 44.5 & t < 0 \\ 50.0 & t > 0 \end{cases} \quad T_{c0} = \begin{cases} 25.0 & t < 7s \\ 20.0 & t > 7s \end{cases} \tag{39}$$

η is a Gaussian white noise with 0.2 ºC of standard deviation:

$$\eta = 0.2Z \; where \sim N(0,1) \tag{37a}$$

that is, Z a random number obtained from normal distribution with mean 0 and variance 1.

The process control simulations are plotted in Figs 1 and 2 and the error and control integrals calculated by trapezoidal rule from simulation results are listed in Table 1.

Table 1. Characteristics of CCTHE SISO controls with T_{h101} as handle variable.

Control	Parameters	ϕ	$(I_e, I_u)_{r=1(t)ss}$	$(I_e, I_u)_{r=1(t)sim}$	$(I_e, I_u)_{r=5(t)sim}$
	$K_p = 7.8\ \tau_1 = 1s$				(21,14)
Maidi *et al*. (2008)	$\tau = 1.03s$				
$\mathcal{L}_2/\mathcal{D}$	$K_{p11} = 1.7$	1.45	(0.21, 0.03)	(0.20,0.04)	(6.1,1.3)
	$K_{i11} = 3.0^{-1}$				

$(I_e, I_u)_{r=1(t)ss}$ integrals defined in (11) and (12) evaluated with (13) and (14) with $K = 1$.
$(I_e, I_u)_{r=1(t)sim}$ same integrals evaluated with trapezoidal rule from simulation with $K = 1$.
$(I_e, I_u)_{r=5(t)sim}$ same integrals evaluated with trapezoidal rule from simulation with $K = 5$.

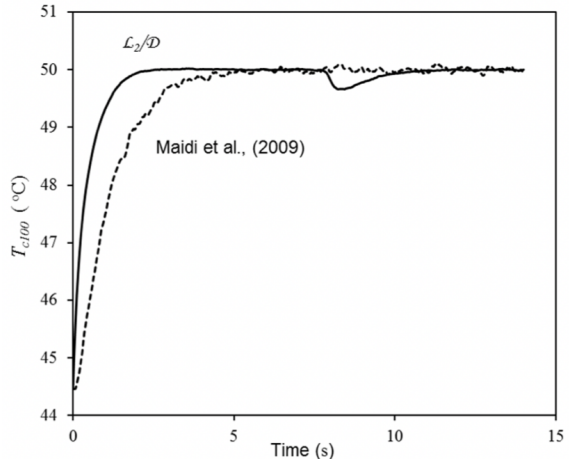

Fig. 1. Target variable evolution (T_{c100}) of CCTHE SISO control with hot fluid temperature (T_{h101}) as control handle variable. $\mathcal{L}_2/\mathcal{D}$ continuous line; Maidi *et al*. (2009) discontinuous line.

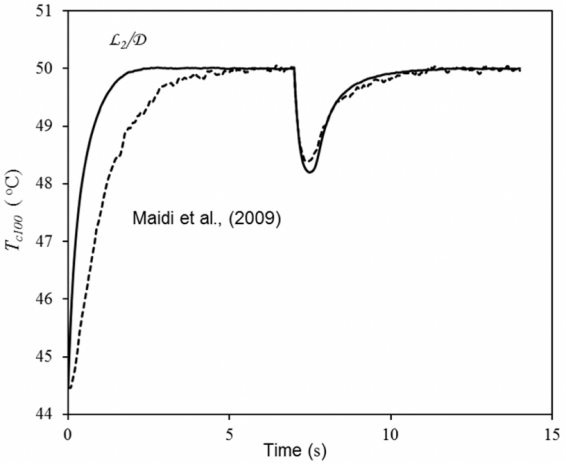

Fig. 3. Target variable evolution (T_{c100}) of CCTHE SISO control with hot fluid temperature (T_{h101}) as control handle variable and inputs (39a). $\mathcal{L}_2/\mathcal{D}$ continuous line; Maidi *et al*. (2009) discontinuous line.

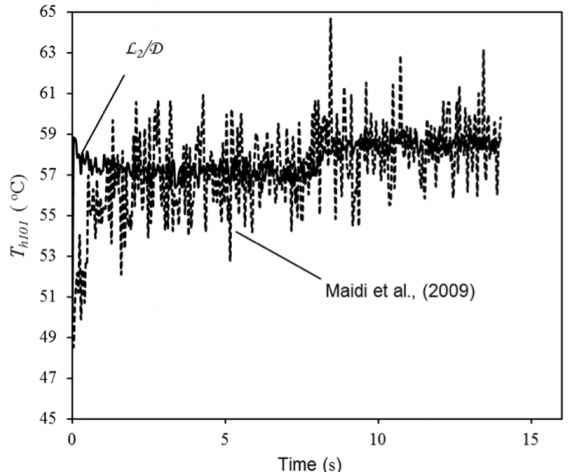

Fig. 2. Control handle variable evolution (T_{h101}) of CCTHE SISO control with hot fluid temperature as control handle variable. $\mathcal{L}_2/\mathcal{D}$ continuous line; Maidi *et al*. (2009) discontinuous line.

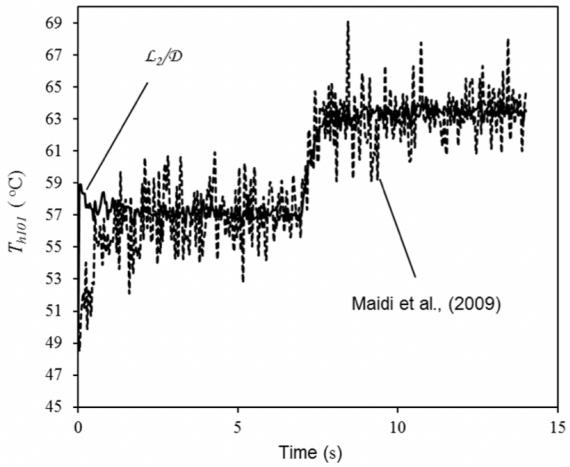

Fig. 4. Control handle variable evolution (T_{h101}) of CCTHE SISO control with hot fluid temperature as control handle variable and inputs (39a). $\mathcal{L}_2/\mathcal{D}$ continuous line; Maidi *et al*. (2009) discontinuous line.

It is evident that for tracking problem the $\mathcal{L}_2/\mathcal{D}$ PI geometric control performs better than Maidi's geometric control (as can be appreciated in Table 1 integrals), otherwise in the regulatory problem Maidi's geometric control performs better than $\mathcal{L}_2/\mathcal{D}$ PI geometric control. Resuming both controls have good performance but the proposed requires only two parameters and does not require the evaluation of a first derivative.

The geometric characteristic ϕ and simultaneous minimization of $\int_0^\infty e'Qedt$ and $\int_0^\infty u'_d Ru_d dt$ improves the robustness and the capacity of reject noise, as can be observed in both Figs. 1 and 2, and it was theoretically justified by Ruiz-López *et al*. (2006) and Voßwinkel *et al*. (2019). In this case we can keep $\phi < \pi/2$ as recommended Voßwinkel *et al*. (2019). Other indications on $\mathcal{L}_2/\mathcal{D}$ PI robustness are the integrals results listed in Table 1. The integrals analytically calculated with Eqs. (1)-(14) and therefore with linearized space-state and $N = 20$ have practically the same value than those numerically obtained with non-linear equations (32) and (33) and $N = 100$. These results demonstrate that geometric $\mathcal{L}_2/\mathcal{D}$ PI algorithm preserves performance even with parameters uncertainties.

The geometric $\mathcal{L}_2/\mathcal{D}$ PI algorithm robustness was additionally tested with the most extreme parameters variations suggested by Maidi *et al*. (2009). These perturbations were introduced as the following input variations,

$$r = \begin{cases} 44.5 & t < 0 \\ 50.0 & t > 0 \end{cases} \quad a_c = \begin{cases} 2.92 & t < 7s \\ 2.34 & t > 7s \end{cases}$$

$$\nu_c = \begin{cases} 1.0 & t < 7s \\ 1.4 & t > 7s \end{cases} \quad a_h = \begin{cases} 5.0 & t < 7s \\ 4.0 & t > 7s \end{cases}$$

$$\nu_h = \begin{cases} 2.0 & t < 7s \\ 2.8 & t > 7s \end{cases} \tag{39a}$$

Both controls simulation were plotted in Figs. 3 and 4. It is evident that geometric $\mathcal{L}_2/\mathcal{D}$ PI algorithm has similar performance than Maidi *et al*. (2009) bounded geometric control, with better capacity for reject noise and with two parameters.

4.2 SISO control with input hot fluid velocity as control handle variable

The $\mathcal{L}_2/\mathcal{D}$ PI characteristics (for matrices 24), for the CCTHE described in section 4.1., tuning by procedure described in section 3 are listed in Table 2. Integrals results listed in Table 2 demonstrate that $\mathcal{L}_2/\mathcal{D}$ PI geometric control performs with the same robustness capacity discussed for Eq. (39) inputs. In this case Maidi *et al*. (2009) did not provide β_1 and β_2 parameters. Therefore, the process simulation was performed only with $\mathcal{L}_2/\mathcal{D}$ PI control by solving Eqs. (32) and (33) with $N = 100$ (and with same initial conditions calculated in 4.1. section) jointly the following control Eqs.
Eqs. 5 and 6 with matrices 24,

$$\frac{d\xi}{dt} = r - (T_{c100} + \eta) \tag{40}$$

$$\nu_h = \nu_{hs} + K_{p22}(r - (T_{c100} + \eta)) + K_{i22}\xi \tag{41}$$

where μ is Gaussian white noise and the inputs are,

$$r = \begin{cases} 44.5 & t < 0 \\ 50.0 & t > 0 \end{cases} \quad T_{c0} = \begin{cases} 25.0 & t < 14s \\ 20.0 & t > 14s \end{cases} \tag{42}$$

Table 2. Characteristics of CCTHE SISO control with ν_h as handle variable

Parameters	ϕ	$(I_e, I_u)_{r=1(t)ss}$	$(I_e, I_u)_{r=1(t)sim}$	$(I_e, I_u)_{r=5(t)sim}$
$K_{p22} = 0.39m \cdot s^{-1} \cdot C^{-1}$ $K_{i22} = 0.69m \cdot s^{-1} \cdot C^{-1}$	1.30	(0.43, 0.02)	(0.51, 0.02)	(2.3, 0.05)

$(I_e, I_u)_{r=1(t)ss}$ integrals defined in (11) and (12) evaluated with (13) and (14) with $K = 1$.
$(I_e, I_u)_{r=1(t)sim}$ same integrals evaluated with trapezoidal rule from simulation with $K = 1$.
$(I_e, I_u)_{r=5(t)sim}$ same integrals evaluated with trapezoidal rule from simulation with $K = 2$.

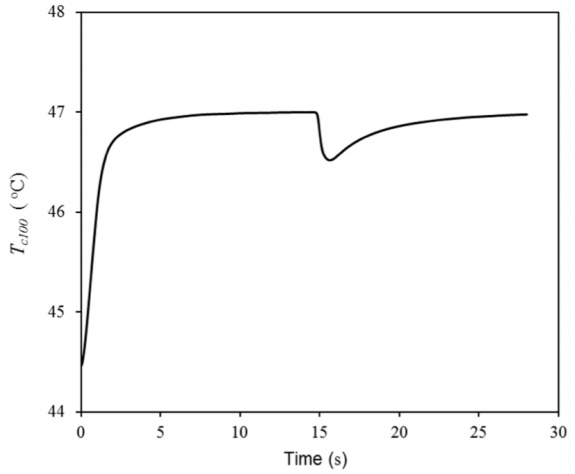

Fig. 5. Target variable evolution (T_{c100}) of CCTHE SISO control with hot fluid velocity (V_h) as control handle variable.

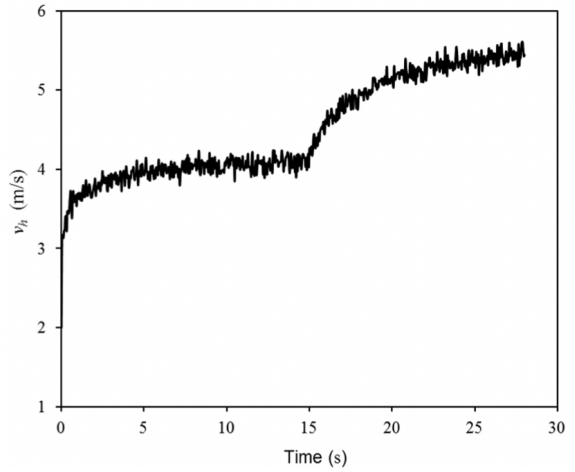

Fig. 6. Control handle variable evolution (V_h) of CCTHE SISO control with hot fluid velocity as control handle variable.

The simulation results are plotted in Figs. 5 and 6. Like it was not possible the direct comparison with Maidi *et al*. (2009) geometric control, some dynamic characteristic will be compared. $\mathcal{L}_2/\mathcal{D}$ PI control had 6 second of stabilizing time in tracking problem while Maidi *et al*. (2009) geometric control had 5 second; $\mathcal{L}_2/\mathcal{D}$ PI control had 9 seconds of stabilizing time in regulator problem while Maidi *et al*. (2009) geometric control had 6 seconds; $\mathcal{L}_2/\mathcal{D}$ PI control had an overresponse of 0.6 ºC second in regulator problem while Maidi *et al*. (2009) had 0.4 ºC. That is, the performance of Maidi *et al*. (2009) was better than proposed $\mathcal{L}_2/\mathcal{D}$ PI algorithm, but with four parameters and with the necessity of first and second derivatives evaluation (Eq. 28). Geometric $\mathcal{L}_2/\mathcal{D}$ PI algorithm had good performance with good noise reject, with only two parameters and without first and second derivatives evaluation.

4.3 MIMO control with input hot fluid temperature and flow as control handle variables

The expansion of CCTHE geometric $\mathcal{L}_2/\mathcal{D}$ PI algorithm to decentralized MIMO structure is natural. Actually, Eqs. (5) and (6) with matrices (21) represent the geometric $\mathcal{L}_2/\mathcal{D}$ PI MIMO algorithm. These Eqs. are particularly written (including Gaussian white noise) as,

$$\frac{d\xi_1}{dt} = r_1 - (T_{c20} + \eta) \tag{43}$$

$$\frac{d\xi_2}{dt} = r_2 - (T_{h1} + \eta) \tag{44}$$

$$\begin{aligned} T_{h21} = T_{h21s} &+ K_{p11}(r_1 - (T_{c20} + \eta)) + K_{i11}\xi_1 \\ &+ K_{p12}(r_2 - (T_{h1} + \eta)) + K_{i12}\xi_2 \end{aligned} \tag{45}$$

$$\begin{aligned} q_h = q_{hs} &+ K_{p21}(r_1 - (T_{c20} + \eta)) + K_{i21}\xi_1 \\ &+ K_{p22}(r_2 - (T_{h1} + \eta)) + K_{i22}\xi_2 \end{aligned} \tag{46}$$

In this case a pilot plant CCTHE with following characteristics were modeled: d_0 = 0.228 dm, d_{01} = 0.251 dm, d_1 = 0.38 dm, L = 58.3 dm, h = 18.4 W·dm^{-2}·ºC^{-1}, Cp = 4185 J·kg^{-1}·ºC^{-1}, ρ =1kg·dm^{-3}, q_c = 0.23dm^3·s^{-1}, q_{hs} = 0.237 dm^3·s^{-1}, T_{c0}=27 ºC, T_{hN+1s} = 57 ºC. In this case the Gaussian white noise was $\eta = 0.1Z$. Eqs. (17) and (18) were solved with N = 20 and the above variables until steady state in order to obtain the initial conditions. $\mathcal{L}_2/\mathcal{D}$ PI MIMO controls were tuned by procedure detailed in Section 3. Eqs. (5) and (6) with matrices (21) (or Eqs. 43 to 46) including decoupling effect ($K_{p12}, K_{p21}, K_{i12}, K_{i21}$). In order to include this decoupling effect during the optimization problem, two groups of integrals were calculated,

$$I_{e1} = \int_0^\infty e'Qedt = K'\mathbf{B}_2'P_y\mathbf{B}_2K \ for\ w = 0,\ K' = [1,0] \tag{47}$$

$$I_{u1} = \int_0^\infty u_d'Ru_ddt = K'\mathbf{B}_2'P_u\mathbf{B}_2K \ for\ w = 0,\ K' = [1,0] \tag{48}$$

Table 3. Characteristics of the CCTHE $\mathcal{L}_2/\mathcal{D}$ PI MIMO controls.

Parameters[a]	ϕ	$(I_e, I_u)_{r=[1(t)\ 0]ss}$ $(I_e, I_u)_{r=[0\ 1(t)]ss}$	$(I_e, I_u)_{r=[1(t)\ 0]sim}$ $(I_e, I_u)_{r=[0\ 1(t)]sim}$
$K_{p11} = 3.5\ K_{p22} = 0.36$	2.6	(2.96, 1.56)	(0.456, 3.87)
$K_{i11} = 0.58\ K_{i22} = 0.67$		(2.60, 2.17)	(0.429,5.39)
$K_{p12} = -0.94\ K_{p21} = 0.26$			
$K_{i12} = -2.0\ K_{p22} = 0.11$			
$K_{p11} = 4.3\ K_{p22} = 0.49$	5.9	(3.1, 0.76)	(2.7, 1.4)
$K_{i11} = 0.91\ K_{i22} = 0.09$		(0.33, 0.71)	(0.26, 1.8)
$K_{p12} = -1.4\ K_{p21} = -0.01$			
$K_{i12} = -2.9\ K_{i22} = -0.005$			

a: K_{p1i} is dimensionless; K_{p2i} has $dm^3 \cdot s^{-1}.^oC^{-1}$ units; K_{i1i} has s^{-1} units; K_{i2i} has $dm^3 \cdot s^{-2}.^oC^{-1}$ units.
ss integrals defined in (11) and (12) evaluated with (13) and (14) with $K = 1$.
sim integrals evaluated with trapezoidal rule from simulation with $K = 1$.

$$I_{e2} = \int_0^\infty e'Qedt = K'\mathbf{B}_2'P_y\mathbf{B}_2K \ for\ w = 0,\ K' = [0,1] \tag{49}$$

$$I_{u2} = \int_0^\infty u_d'Ru_ddt = K'\mathbf{B}_2'P_u\mathbf{B}_2K \ for\ w = 0,\ K' = [0,1] \tag{50}$$

And the section 3.3. problem was solved with,

$$minI(\alpha,\beta_1,\beta_2,\gamma,\delta_1,\delta_2) = I_{e1} + I_{u1} + I_{e2} + I_{u2} \tag{51}$$

as target function.

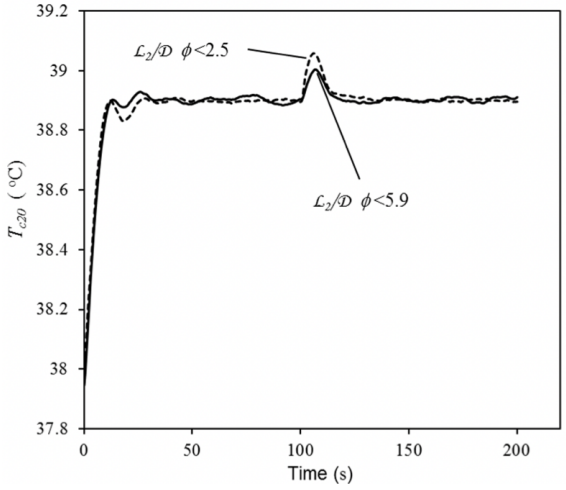

Fig. 7. T_{c20} evolution of CCTHE MIMO $\mathcal{L}_2/\mathcal{D}$ control. $\phi < 5.8$ continuous line; $\phi < 2.6$ discontinuous line.

Like there are not previous reported controls for comparison, two possible solutions for $\mathcal{L}_2/\mathcal{D}$ PI MIMO controls were reported in Table 3. In this case it was not possible to keep $\phi < \pi/2$ and the first solution was obtained with $\phi < 2.6$. Even that, this constrain for $\mathcal{D}$ region limits the minimization of I_{u1} and I_{u2} variables. Therefore, in the second solution the constrain was relaxed to $\phi < 5.9$, which allowed to decrease the cited integrals (Table 3). Result listed in Table 3 leads to remark 5.

Remark 5 □ *In Table 3 results can be observed that like $I_{e1} \in \mathcal{L}_2$, $I_{e2} \in \mathcal{L}_2$, $I_{u1} \in \mathcal{L}_2$ and $I_{u2} \in \mathcal{L}_2$, the integrals can be reduced simultaneously in the minimization of $I = I_{e1} + I_{u1} + I_{e2} + I_{u2}$. Instead, the typical action control square integral is competitive with error square integral. Table 3 results represent a case in which I_{e1}, I_{e2}, I_{u1} and I_{u2} are non-competitive.*□

The two solutions were simulated with,

$$r = \begin{cases} 37.9 & t < 0 \\ 38.9 & t > 0 \end{cases} \quad T_{c0} = \begin{cases} 39.1 & t < 100s \\ 40.1 & t > 100s \end{cases} \tag{52}$$

The results are plotted in Figs. 7 to 10. Both solutions had similar behaviors in the first target variable (T_{c20}), but the $\phi < 5.9$ control performs better for the second target variable (T_{h1}). The noise in control actions (Figs. 9 and 10) were closely but with a bit better rejection capacity by $\phi < 5.9$ control. That is, the reduction of I_{u1} and I_{u2} integrals guaranties the noise rejection. The robustness of proposed $\mathcal{L}_2/\mathcal{D}$

PI MIMO geometric control can be appreciated in integrals listed in Table 3. The integrals analytically solved with Eqs. (47)-(50) and linearized model have even greater value than those obtained numerically with non-linear model (Eqs. 17 and 18). This result demonstrates that $\mathcal{L}_2/\mathcal{D}$ PI MIMO geometric control holds the performance even with uncertainness in parameters.

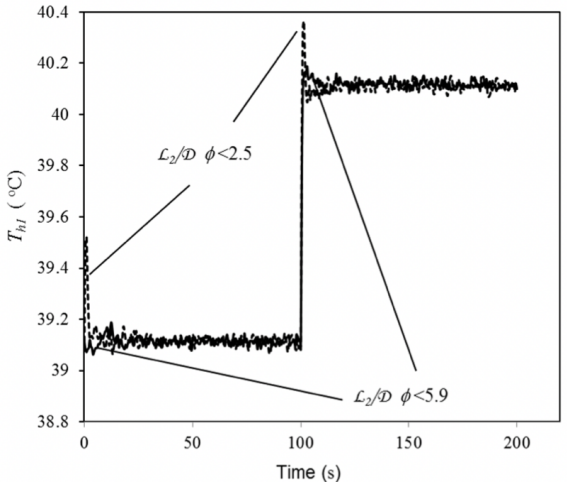

Fig. 8. T_{h1} evolution of CCTHE MIMO $\mathcal{L}_2/\mathcal{D}$ control. $\phi < 5.8$ continuous line; $\phi < 2.6$ discontinuous line.

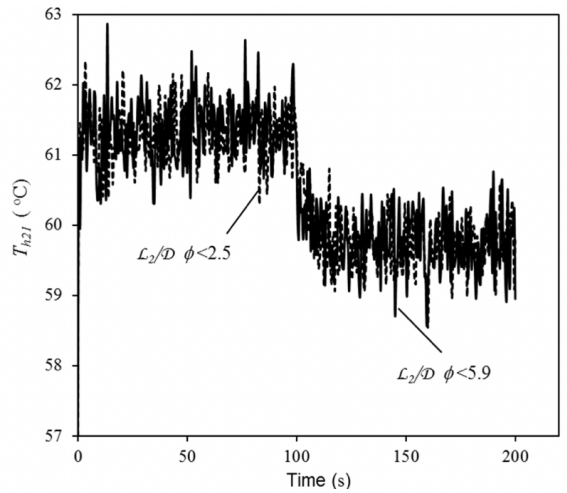

Fig. 9. T_{h21} evolution (first handle control variable) of CCTHE MIMO $\mathcal{L}_2/\mathcal{D}$ control. $\phi < 5.9$ continuous line; $\phi < 2.6$ discontinuous line.

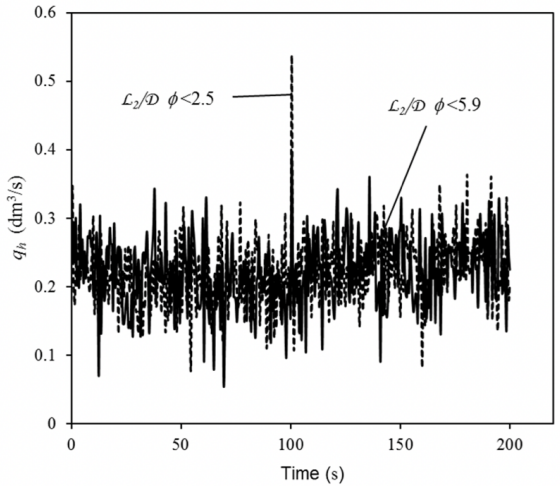

Fig.10. q_h evolution (second handle control variable) of CCTHE MIMO $\mathcal{L}_2/\mathcal{D}$ control. $\phi < 5.9$ continuous line; $\phi < 2.6$ discontinuous line.

Conclusions

It was demonstrated that problem defined in Eqs. (1) to (7) represents a non-competitive $\mathcal{L}_2/\mathcal{D}$ parametric geometric control, which improve the potential (described in remarks 1-5) of any control algorithm that can be represented by this problem as optimal-robust control. The tuning algorithm based on this definition found two sets of parameters duple (K_p, K_i) under $\mathcal{L}_2/\mathcal{D}$ PI SISO criterion (as examples of linear control algorithms), for continuous concentric tubes heat exchanger (CCTHE) with similar performance and robustness than other geometric controls with three and four parameters. The $\mathcal{L}_2/\mathcal{D}$ PI algorithm was easily extended to a CCTHE decentralized MIMO control. The CCTHE MIMO $\mathcal{L}_2/\mathcal{D}$ control was an example in which errors integrals vs control signals were non-necessarily competitive like it was stated in remark 2.

Acknowledgements

Authors express their acknowledge to Mexican Consejo Nacional de Ciencia y Tecnología (CONACyT) by financial support through the project CB-2011-01-166977, and by the scholarship for González, R. and Flores-Márquez, J.A.

References

Alzate-Ibanez, A.M. (2018). States and variables estimation in an upflow anaerobic sludge blanket reactor for the leachate waste water treatment using non-linear observers. *Revista Mexicana de Ingeniería Química 17*, 723-738.

Aguilar-Garnica, E., García-Sandoval, J.P. González-Alvarez, V. (2011). PI controller design for a class of distributed parameter systems. *Chemical Engineering Science 66*, 4009-4019.

Bolaños-Reynoso, E., Sánchez-Sánchez, K., López-Zamora, L., Ricardez-Sandoval, L. (2018). A study on empirical and mechanistic approaches for modelling cane sugar crystallization. *Revista Mexicana de Ingeniería Química 17*, 389-407.

Boscain, U.; Piccoli, B. (1998). Geometric control approach to synthesis theory. *Rendiconti del Seminario Matematico Università e Politecnico di Torino 56*, 53-68.

Carrillo-Ahumada, J., Rodriguez-Jimenes, G.C., García-Alvarado, M.A. (2011). Tuning optimal-robust linear MIMO controllers of chemical reactors by using Pareto optimality. *Chemical Engineering Journal 174*, 357-367.

Carrillo-Ahumada, J. Reynoso-Meza, G., García-Nieto, S., Sanchis, J., García-Alvarado, M.A. (2015). Sintonización de controladores Pareto-óptimo robustos para sistemas multivariables. *Aplicación en un helicóptero de 2 grados de libertad. Revista Iberoamericana de Automática Industrial 12*, 177-188.

Chen, C.L., Wang, T.C., Hsu, S.H. (2002). An LMI approach to H PI controller design. *Journal of Chemical Engineering Japan 35*, 83-93.

Estévez-Sánchez, K.H., Sampieri-Croda, A., García-Alvarado, M.A., Ruiz-López, I.I. (2017). Design of multiloop PI controllers based on quadratic optimal approach. *ISA Transactions 70*, 338-347.

García, J., Fernandez-Anaya, G., Vargas-Villamil, F.D. Orduña, E. (2010). Estructura de control jerarquico aplicada a un reactor de amoniaco, tipo tubular, con enfriamiento intermedio. *Revista Mexicana de Ingeniería Química 9*, 329-341.

García-Alvarado, M.A., Ruiz-Lopez, I.I. (2010). A design method for robust and quadratic optimal MIMO linear controllers. *Chemical Engineering Science 65*, 3431-3438.

Goncalves, E.N., Palhares, R.M., Takahashi, R.H.C. (2008). A novel approach for H2/Hinf robust PID synthesis for uncertain systems. *Journal of Process Control 18*, 19-26.

Hernández-Martínez, Urrea, E. R., Álvarez-Ramírez, J. (2008). Mejora en el control en cascada para reactores tubulares. *Revista Mexicana de Ingeniería Química 7*, 309-318. Juarez-Romero, D., Lopez-Estrada, F.R., Astorga-Zaragoza, C.M., Alvarado, V., Hernandez, J.A. and Tellez-

Anguiano, A.C. (2010). Modeling the configuration characteristics and operating regimes of a binary distillation column for control. *Revista Mexicana de Ingeniería Química 9*, 367-382.

Ma, D., Chen, J., Liu, A., Chen, J., Niculescu, S.I. (2019). Explicit bounds for guaranteed stabilization by PID control of second-order unstable delay systems. *Automatica 100*, 407-411.

Maidi, A., Diaf, M., Corriou, J.P. (2009). Boundary geometric control of a counter-current heat exchanger. *Journal of Process Control 19*, 297-313.

Martínez-Monteagudo, S.I. (2018). Analysis of thermoxidation kinetics of milk fat. *Revista Mexicana de Ingeniería Química 17*, 587-602.

Kozakova, A., Vesely, V., Kučera, V. (2019). Robust decentralized controller design based on equivalent subsystems. *Automatica 107*, 19-35.

Ruiz-López, I.I., Rodríguez-Jimenes, G.C., García-Alvarado, M.A. (2006). Robust MIMO PID controllers tuning based on complex/real ratio of the characteristic matrix eigenvalues. *Chemical Engineering Science 61*, 4332-4340.

Schorsch, J., Castro, C.C., Couto, L.D., Nobre, C., Kinnaert, M. (2019). Optimal control for fermentative production of fructo-oligo saccharides in fed-batch bioreactor. *Journal of Process Control 78*, 124-138

Shih, Y.P. (1969). Optimal control of distributed-parameters system with integral equation constrains. *Chemical Engineering Science 24*, 671-680.

Tsiligiannis, C.A., Svoronos, S.A. (1988). Dynamic interactors in multivariable process control-I. The general time delay case. *Chemical Engineering Science 43*, 339-347.

Vargas-González, S., Rodriguez-Jimenes, G.C, García-Alvarado, M.A., Carrillo-Ahumada, J. (2013). Relation between first order dynamic parameters with PI control parameters in Nash equilibrium. Proceedings - 2013 International Conference on Mechatronics, Electronics and Automotive Engineering, ICMEAE 2013. DOI: 10.1109/ICMEAE.2013.21.

Velasco-Pérez, A., Alvarez-Ramírez, J.A. and Solar-González, R. (2011). Control multiple entrada una salida (MISO) de un CSTR. *Revista Mexicana de Ingeniería Química 10*, 321-331.

Voßwinkel, R., Pyta, L., Schrodel, F., Mutlu, I., Mihailescu-Stoica, D., Bajcinca, N. (2019). Performance boundary mapping for continuous and discrete time linear systems. *Automatica 107*, 272-280.

Xie,S., Xie, Y., Yang, C., Gui, W., Wang, Y. (2018). Distributed parameter modeling and optimal control of the oxidationrate in the iron removal process. *Journal of Process Control 61*, 47-57.

Appendix A

□ Theorem 1

For system defined with Eqs. (3)-(10) in minimal realization, with a zero pole in α, β_1 β_2, γ, δ_2 *and* δ_2, *and with* $\mathbf{A}$ *Hurwitz,*

$$I_u = \int_0^\infty u_d' R u_d dt = K' \mathbf{B}_2' P_u \mathbf{B}_2 K$$

$$for\ w = 0,\ r = 1(t)K \tag{A.1}$$

where

$$\mathbf{A}' P_u + P_u \mathbf{A} + \left(\mathbf{A}^{-1}\right)' \mathbf{C}_2' R \mathbf{C}_2 \left(\mathbf{A}^{-1}\right) = 0 \tag{A2}$$

Proof

Analytical solution (for matrices with constant elements) of Eq. (8)-(10) is,

$$\mathbf{X} = \mathbf{A}^{-1}\left(e^{\mathbf{A}t} - \mathbf{I}\right)(\mathbf{B}_2 K) \tag{A3}$$

$$y = \mathbf{C}_1 \mathbf{A}^{-1}\left(e^{\mathbf{A}t} - \mathbf{I}\right)(\mathbf{B}_2 K) + \mathbf{D}_{12} K \tag{A4}$$

$$u = \mathbf{C}_2 \mathbf{A}^{-1}\left(e^{\mathbf{A}t} - \mathbf{I}\right)(\mathbf{B}_2 K) + \mathbf{D}_{22} K \tag{A5}$$

Like the system described with Eqs. (3)-(10) is in minimal realization with $\mathbf{A}$ *Hurwitz implies,*

$$\lim_{t\to\infty} \mathbf{C}_1 \mathbf{A}^{-1} e^{\mathbf{A}t} \mathbf{B}_2 K = 0 \text{ and}$$

$$\lim_{t\to\infty} \mathbf{C}_2 \mathbf{A}^{-1} e^{\mathbf{A}t} \mathbf{B}_2 K = 0 \tag{A6}$$

and with a zero pole in α, β_1 β_2, γ, δ_1 *and* δ_2 *(integral action), under a step disturbance the error has not off set* ($e(t) \in \mathcal{L}_{2+}$) *implies,*

$$\lim_{t\to\infty} y = r = K,\ \lim_{t\to\infty} u = u_\infty = -\mathbf{C}_2 \mathbf{A}^{-1} \mathbf{B}_2 K + \mathbf{D}_{22} K \tag{A7}$$

Therefore from A(5), A(6) and (A7),

$$u - u_\infty = \mathbf{C}_2 \mathbf{A}^{-1} e^{\mathbf{A}t} \mathbf{B}_2 K$$

And therefore,

$$I_u = \int_0^\infty u_d' R u_d dt = K' \mathbf{B}_2' \int_0^\infty \left(e^{\mathbf{A}t}\right)' \left(\mathbf{A}^{-1}\right)' \mathbf{C}_2' R \mathbf{C}_2 \mathbf{A}^{-1} e^{\mathbf{A}t} dt \mathbf{B}_2 K \tag{A8}$$

By the other hand, $\Theta = e^{\mathbf{A}t}$ *is the solution of,*

$$\frac{d\Theta}{dt} = \mathbf{A}\Theta \ \ with\ \ \Theta(t) = \mathbf{1} \tag{A9}$$

Lyapunuv function of Eq. (A9) is $V(t) = \Theta' P_u \Theta$ *and its derivative,*

$$\dot{V}(t) = \Theta'(\mathbf{A}' P_u + P_u \mathbf{A})\Theta = \Theta' \mathbf{R} \Theta \tag{A10}$$

Like $\mathbf{A}$ *is Hurwitz* $\dot{V}(t) \leq 0 \; \forall t$ *or,*

$\mathbf{A}' P_u + P_u \mathbf{A} = -\mathbf{R}$ *where* $\mathbf{R}$ *is positive definite* (A11)

Defining from (A8) $\mathbf{R} = \left(\mathbf{A}^{-1}\right)' \mathbf{C}_2' R \mathbf{C}_2 \left(\mathbf{A}^{-1}\right)$ *and from (A11),*

$$\int_0^\infty \left(e^{\mathbf{A}t}\right)' \left(\mathbf{A}^{-1}\right)' \mathbf{C}_2' R \mathbf{C}_2 \mathbf{A}^{-1} e^{\mathbf{A}t} dt = -\int_0^\infty \Theta' \mathbf{R} \Theta dt = \int_0^\infty \dot{V}(t) dt = -V(t)_0^\infty = P_u \tag{A12}$$

which proof the theorem.□